J. Mater. Environ. Sci. 7 (10) (2016) 3916-3929
ISSN : 2028-2508
CODEN: JMESCN

Density Functional Theory modeling and Monte Carlo simulation assessment of N-Substituted Quinoxaline Derivatives as Mild Steel Corrosion Inhibitors in acidic medium

Y. Karzazi[1, 2, *], M. E. Belghiti[1], F. El-Hajjaji[3] and B.Hammouti[1]
[1] *Laboratory of Applied Analytical Chemistry Materials and Environment (LA2AME), Faculty of Sciences, University Mohammed Premier, P. O. Box 4808, 60046 Oujda, Morocco*
[2]*LSIA, National School of Applied Sciences, ENSA Al Hoceima, University Mohammed Premier, P. O. Box 3, 32003 Sidi Bouafif, Morocco*
[3] *Laboratoire d'Ingénierie d'Electrochimie, Modélisation et d'Environnement (LIEME), Faculty of Sciences, University Sidi Mohammed Ben Abdellah, Fez, Morocco*

Received 31 Apr 2016, Revised 23 Jul 2016, Accepted 27 July 2016
**For correspondence: Email: karzazi@hotmail.com*

Abstract
This work attempts to correlate the structural and electronic properties, such as HOMO, LUMO energy values, frontier orbital energy gap, molecular dipole moment (μ), electron affinity (A), ionization potential (I), electronegativity (χ), global hardness (η), softness (σ), the fraction of electron transferred (ΔN), electrophilicity index (ω), back-donation (ΔEback-donation) and Mulliken charges using density functional theory (DFT) at the B3LYP/6-31G(d,p) basis set, with the inhibitive action of two quinoxaline derivatives named: 3-methyl-1-prop-2-ynylquinoxalin-2(1H)-one (Pr-N-Q=O) and 3-methyl-1-prop-2-ynylquinoxaline-2(1H)-thione (Pr-N-Q=S), of the mild steel corrosion in molar hydrochloric acid. Monte Carlo simulations were further performed to simulate the adsorption of the two quinoxaline derivatives on Fe (111) surface in the presence of water and the results show that Pr-N-Q=S is the most effective as corrosion inhibitor for mild steel in 1 M HCl medium.

Keywords:Corrosion; Inhibition; Mild steel; HCl medium; DFT; Electronic properties; Monte Carlo simulation.

1. Introduction
Mild steel is widely employed in industry because of its low cost and availability. As a result of its industrial concern, attention has been paid to study and to prevent this metal against corrosion in aggressive environments [1-3]. Acid solutions are generally used for the removal of undesirable scale and rust in several industrial areas such as acid pickling, acid descaling, acid cleaning of boilers, and oil well acidizing [4-6]. Because of the general aggressiveness of acids, inhibitors are often used to control the metal dissolution as well as the acid consumption reducing by the way the overall corrosion current density [7-11]. Inhibitors are adsorbed on the metal surface, forming a protective barrier and interact with anodic or/and cathodic reaction sites to decrease the oxidation or/and reduction of corrosion reactions. The inhibition of corrosion in acid solutions can be secured by the addition of a variety of organic compounds containing electronegative functional groups and π electrons in conjugated double or triple bonds and hence exhibit good inhibitive properties by supplying electrons through π orbitals. There is also a specific interaction between functional groups containing heteroatoms like nitrogen, phosphorus, sulfur and/or oxygen having free lone pair of electrons and the metal surface, which play an important role in inhibition. When both of these features combine, increased inhibition can be observed [12–16]. However, the use of organic inhibitors in acid solutions can, in some cases, lead to enhancement of the metal

corrosion [17], and stimulation of corrosion is correlated not only to the type and structure of the organic molecule but also depends on the type of acid and its concentration [18-21]. The corrosion inhibition, normally considered by corrosion scientists, is the relation between the molecular/electronic structures and corrosion inhibition efficiency. In the last decades, numerous researches were devoted to give more explanation to the obtained efficiency of quinoxaline derivatives to many applications at various fields such as inhibition of corrosion for steel, Aluminum and copper in acidic medium [22-25], anti-viral [26], anti-bacterial [27], anti-inflammatory [28], anti-protozoal [29], anti-cancer [30,31] anti-depressant [32], anti-HIV [33], and as kinase inhibitors [34]. They are also used in the agricultural field as fungicides, herbicides, and insecticides [35].In the present work, the correlation between inhibition efficiency and molecular structure of two quinoxaline derivatives (Figure 1) is investigated by determination of chemical indexes, which were performed using density functional theory (DFT) at the B3LYP/6-31G(d,p) level. To the best of our knowledge, connection between the structural parameters and corrosion inhibition of these compounds has not been reported in open literature.

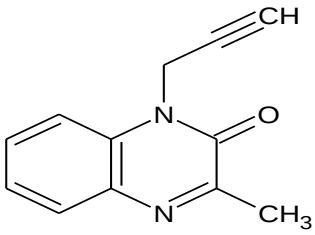

3-methyl-1-prop-2-ynylquinoxalin-2(1H)-one
Pr-N-Q=O

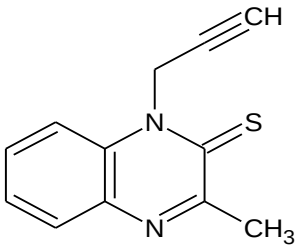

3-methyl-1-prop-2-ynylquinoxaline-2(1H)-thionePr-N-Q=S

Figure 1. The chemical structures of investigated inhibitors (Pr-N-Q=O and Pr-N-Q=S).

2. Molecular simulations and quantum chemical calculations

2.1. Theory and computational details

Quantum chemical calculations have been proved to be a powerful tool for studying corrosion inhibition mechanism [36-38]. Density Functional theory (DFT), based on Beck's three parameter exchange functional and Lee–Yang–Parr nonlocal correlation functional (B3LYP) [39-41] and the 6-31G(d, p) orbital basis sets for all atoms as implemented in Gaussian 09 program [42], was performed on Pr-N-Q=O and Pr-N-Q=S in order to describe the interaction between the inhibitors molecules and the surface as well as the properties of these inhibitors concerning their reactivity. Hence, the geometries of molecules under study, in aqueous phase, were fully optimized with no constraints using DFT at the B3LYP/6-31G(d,p) level. All the calculations were performed in the presence of a solvent (water) by placing the solute in a cavity within the solvent reaction field. The Polarizable Continuum Model (PCM) using the integral equation formalism variant (IEFPCM) which is a self-consistent reaction field (SCRF) was used for water phase calculations [43]. Hereafter, we have investigated the relationship between the molecular, the electronic structure and the inhibition efficiency of the two studied molecules. For these seek, some molecular descriptors most relevant to their potential action as corrosion inhibitors, such as HOMO and LUMO energy values, frontier orbital energy gap, molecular dipole moment (μ), electron affinity (A), ionization potential (I), electronegativity (χ), global hardness (η), softness (σ), the fraction of electron transferred (ΔN), electrophilicity index (ω) and back-donation ($\Delta E_{back\text{-}donation}$), were calculated using the DFT method and have been used to understand the properties and activity of the newly prepared compounds and to help in the explanation of the experimental data obtained for the corrosion process.

The frontier orbital HOMO and LUMO of a chemical species are very important in defining its reactivity. A good correlation has been found between the speeds of corrosion and E_{HOMO} that is often associated with the electron donating ability of the molecule. Survey of literature shows that the adsorption of the inhibitor on the metal surface can occur on the basis of donor–acceptor interactions between the π-electrons of the heterocyclic compound and the vacant d-orbital of the metal surface atoms [44].], high value of E_{HOMO} of the molecules shows

its tendency to donate electrons to appropriate acceptor molecules with low energy empty molecular orbitals. Increasing values of E_{HOMO} facilitate adsorption and therefore enhance the inhibition efficiency, by influencing the transport process through the adsorbed layer. Similar relations were found between the rates of corrosion and ΔE ($\Delta E = E_{LUMO} - E_{HOMO}$) [43, 45-46]. The energy of the lowest unoccupied molecular orbital indicates the ability of the molecule to accept electrons. The lower the value of E_{LUMO}, the more probable the molecule would accept electrons. Consequently, concerning the value of the energy gap ΔE, larger values of the energy difference will provide low reactivity to a chemical species. Lower values of the ΔE will render good inhibition efficiency, because the energy required to remove an electron from the lowest occupied orbital will be low [47]. Another method to correlate inhibition efficiency with parameters of molecular structure is to calculate the fraction of electrons transferred from inhibitor to metal surface. According to Koopman's theorem [48], E_{HOMO} and E_{LUMO} of the inhibitor molecule are related to the ionization potential (I) and the electron affinity (A), respectively. The ionization potential and the electron affinity are defined as $I = -E_{HOMO}$ and $A = -E_{LUMO}$, respectively. Then absolute electronegativity (χ) and global hardness (η) of the inhibitor molecule are approximated as follows [47]:

$$\chi = \frac{I+A}{2}, \qquad \chi = -\frac{1}{2}(E_{HOMO} + E_{LUMO})$$

$$\eta = \frac{I-A}{2}, \qquad \eta = -\frac{1}{2}(E_{HOMO} - E_{LUMO})$$

As hardness (η), softness (S) is a global chemical descriptor measuring the molecular stability and reactivity and is given by:

$$S = \frac{1}{\eta}, \qquad S = -2/(E_{HOMO} - E_{LUMO})$$

The chemical hardness fundamentally signifies the resistance towards the deformation or polarization of the electron cloud of the atoms, ions or molecules under small perturbation of chemical reaction. A hard molecule has a large energy gap and a soft molecule has a small energy gap [48]. The global electrophilicity index was introduced by Parr as a measure of energy lowering due to maximal electron flow between donor and acceptor and is given by [49]:

$$\omega = \left(\frac{\mu^2}{2}\right) S, \qquad \omega = \frac{(I+A)}{8}$$

According to the definition, this index measures the propensity of chemical species to accept electrons. A good, more reactive, nucleophilic is characterized by lower value of μ, ω; and conversely a good electrophilic is characterized by a high value of μ, ω. This new reactivity index measures the stabilization in energy when the system acquires an additional electronic charge ΔN from the environment. Thus the fraction of electrons transferred from the inhibitor to metallic surface, ΔN, is given by [50]:

$$\Delta N = \frac{\chi_{Fe} - \chi_{inh}}{2(\eta_{Fe} + \eta_{inh})}$$

Where χ_{Fe} and χ_{inh} denote the absolute electronegativity of iron and inhibitor molecule, respectively; η_{Fe} and η_{inh} denote the absolute hardness of iron and the inhibitor molecule, respectively.

In order to calculate the fraction of electrons transferred, a theoretical value of $\chi_{Fe} = +7.0$ eV [51] and $\eta_{Fe} = 0$ $(eV)^{-1}$ by assuming that for a metallic bulk I = A, because they are softer than the neutral metallic atoms [52]. According to the simple charge transfer model for donation and back donation of charges [53], when a molecule receives a certain amount of charge, $\Delta N+$; then:

$$\Delta E^{+} = \mu + \Delta N^{+} + \frac{1}{2}\eta (\Delta N^{+})^{2} \qquad (a)$$

While when a molecule back-donates a certain amount of charge, $\Delta N-$, then:

$$\Delta E^{-} = \mu^{-} \Delta N^{-} + \frac{1}{2}\eta (\Delta N^{-})^{2} \qquad (b)$$

If the total energy change is approximated by the sum of the contributions of Eqs. (a) and (b), assuming that the amount of charge back-donation is equal to the amount of charge received, $\Delta N^{+} + \Delta N^{-} = 0$, then;

$$\Delta E_T = \Delta E_{back\text{-}donation} = \Delta E^{+} + \Delta E^{-} = (\mu^{+} + \mu^{-})\Delta N^{+} + \frac{1}{2}\eta (\Delta N^{+})^{2} + \frac{1}{2}\eta (\Delta N^{-})^{2}$$

$$\Delta E_{back\text{-}donation} = (\mu^{+} + \mu^{-})\Delta N^{+} + \eta (\Delta N^{+})^{2}; \qquad (\Delta N^{+} = -\Delta N^{-})$$

The most favorable situation corresponds to the case when the total energy change ($\Delta E_{back\text{-}donation}$) becomes a minimum with respect to ΔN^+, which implies that ($\Delta N^+ = -(\mu^+ + \mu^-)/2\eta$) and that;

$$\Delta E_{back\text{-}donation} = -(\mu^+ - \mu^-)^2/4\eta = -\frac{\eta}{4} \qquad \Delta E_{back\text{-}donation} = \frac{1}{8}(E_{HOMO} - E_{LUMO})$$

The $\Delta E_{back\text{-}donation}$ implies that when $\eta > 0$ and $\Delta E_{back\text{-}donation} < 0$ the charge transfer to a molecule, followed by a back-donation from the molecule, is energetically favoured. In this context, hence, it is possible to compare the stabilization among inhibiting molecules, since there will be an interaction with the same metal, then, it is expected that it will decrease as the hardness increases.

2.2. Monte Carlo simulations

The Monte Carlo (MC) search was used to calculate the low configuration adsorption energy of the interactions of two quinoxaline derivativeson clean iron surface. Metropolis Monte Carlo (MC) simulations methodology [54] using the DMol-3 code [55-56]and Adsorption Locator [57-58] implemented in the BOVIA Material Studio 8.0 (Accelrys, San Diego, CA, USA) [59], has been used to build the system adsorbate/substrate. Simulations were carried out with a slab thickness of 5Å, a super cell of (6 × 6) and a vacuum of 30 Å along the C-axis in a simulation box (25.17Å x 25.37Å x 40.26Å) with periodic boundary conditions to model a representative part of the interface devoid of any arbitrary boundary effects. For the whole simulation procedure, the COMPASS force field (condensed-phase optimized molecular potentials for atomistic simulation studies) [60] was used to optimize the structures of all components of the corrosion system (metal substrate / inhibitor / solvent molecules). To mimic the real corrosion environment, 30 molecules of water were added to the simulation box. This computational study aims to find low-energy adsorption sites to investigate the preferential adsorption of inhibitor molecules on iron surface aiming to find a relationship between the effect of its molecular structure and its inhibition efficiency.

3. Results and discussion

3.1. Calculations of the quantum chemical descriptors

The inhibition of mild steel using two quinoxaline derivatives; Pr-N-Q=O and Pr-N-Q=S as corrosion inhibitors were investigated experimentally, the classification of these inhibitors according to their corrosion inhibition efficiency is: Pr-N-Q=S >Pr-N-Q=O (93.4 % > 90 %, respectively) [61]. The high inhibitive performance of Pr-N-Q=S and Pr-N-Q=O suggests a strong bonding of this quinoxaline molecules onto the metal surface due to the existence of several lone pairs from heteroatom (oxygen and sulphur) and π-orbitals, blocking the active sites and hence reducing the corrosion rate. Moreover, the higher inhibition efficiency of Pr-N-Q=S can be attributed to the existence of thioxo group on the quinoxaline ring, which gives the possibility of dπ-dπ bond formation resulting from overlap of 3d electrons from Fe atom and the 3d vacant orbital of sulphur atom [62-64].Accordingly, quantum chemical calculations based on DFT method, at the B3LYP/6-31G(d,p) level, were performed to investigate the effect of structural parameters on the inhibition efficiency of inhibitors and study their adsorption mechanisms on the metal surface. The geometric and electronic structures of Pr-N-Q=S and Pr-N-Q=O in solvent phase (water) were calculated from optimized structures and presented in Fig. 2.

In this work, the optimized geometries with the DFT at the B3LYP/6-31G(d,p) level of the two inhibitors are essentially planar. This may facilitate the donation of π-electrons by the aromatic rings, the nonbinding electron pair of nitrogen and sulphur in quinoxaline molecules as well as the oxo group or the propyne group with triple bond. The ground state geometry of the inhibitor as well as the nature of its frontier molecular orbitals, explicitly, the highest occupied molecular orbital (HOMO) and the lowest unoccupied molecular orbital (LUMO) are involved in the activity properties of the inhibitors. Frontier molecular orbital diagrams of Pr-N-Q=S and Pr-N-Q=O as calculated with the DFT at the B3LYP/6-31G(d,p) level are represented in Fig. 3.

Figure 3 shows that, the HOMO's and LUMO's are strongly delocalized in the conjugated system of the molecules Pr-N-Q=S and Pr-N-Q=O. The contour plots of the HOMO and LUMO are structural dependent and the electron density of the HOMO location in the inhibitors under study is mostly distributed on the atoms having a delocalized character showing that these atoms are the favorite adsorption sites. Note that the strongest

contribution for the HOMO is encountered for the C=S group in Pr-N-Q=S which is the best inhibitor experimentally. Hence, our theoretical results are in good agreement with the experiment.

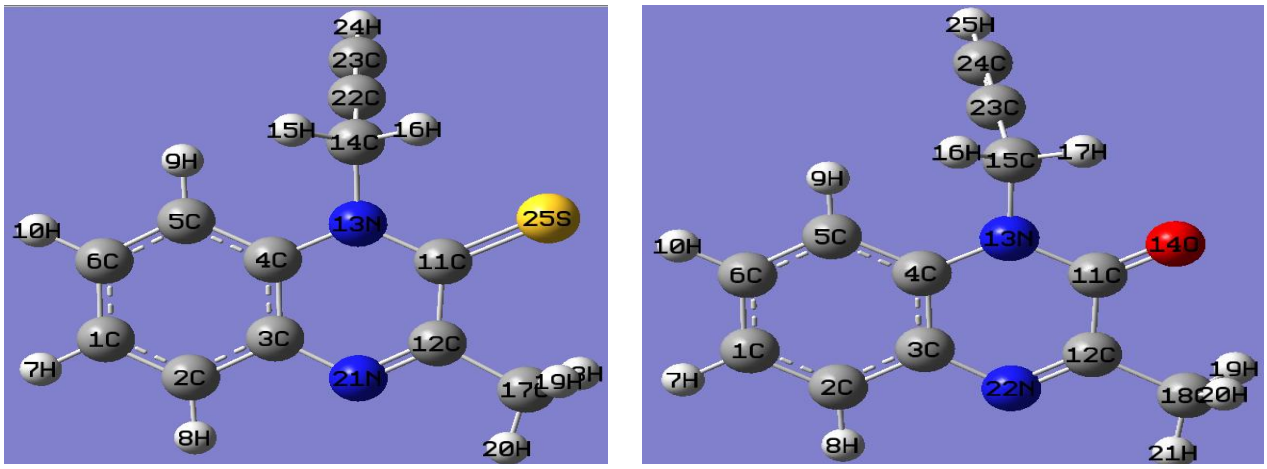

Pr-N-Q=S Pr-N-Q=O

Figure 2. Optimized Structure of Pr-N-Q=S and Pr-N-Q=O calculated in solvent phase (water) at the B3LYP/6-31G(d,p) level.

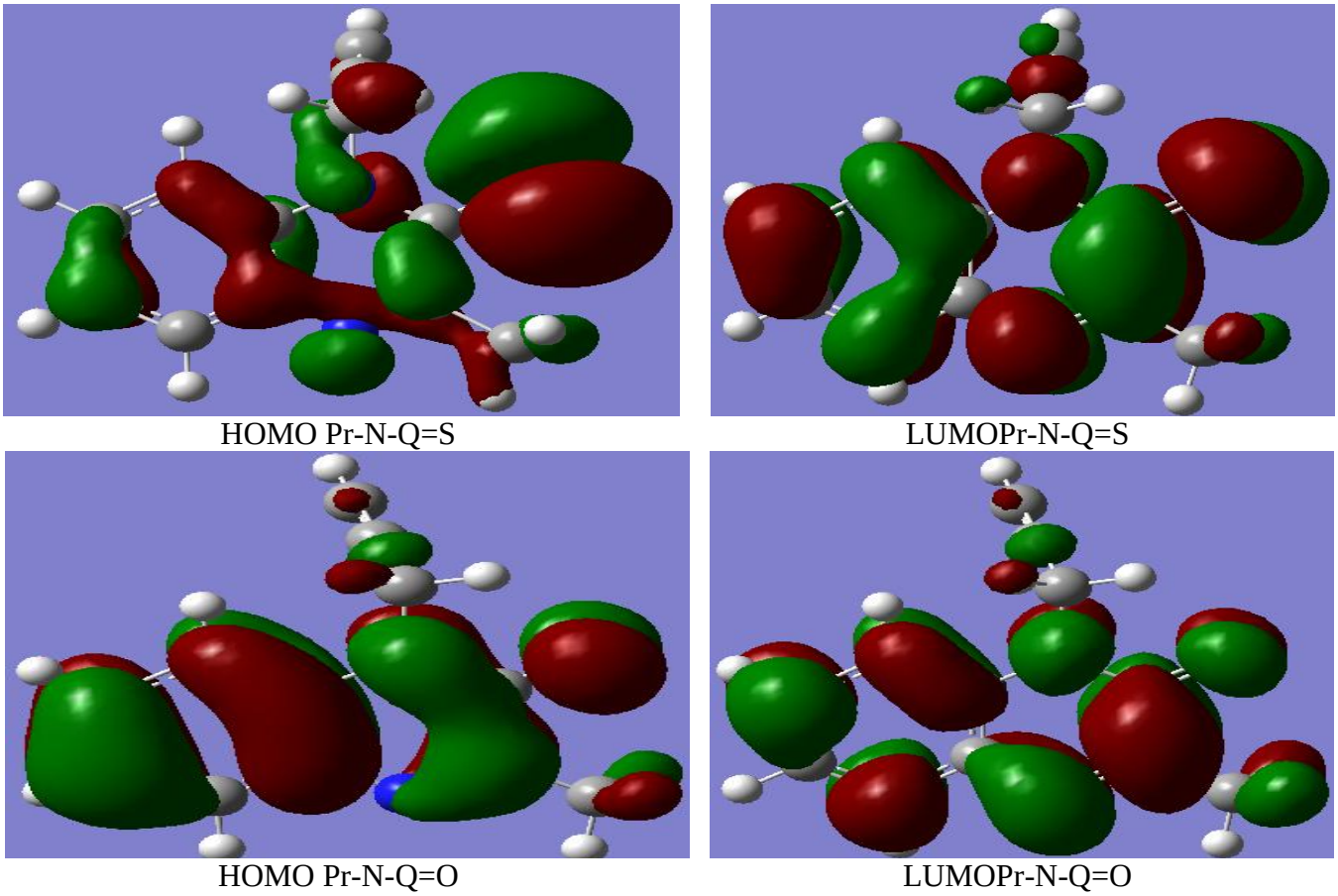

HOMO Pr-N-Q=S LUMOPr-N-Q=S

HOMO Pr-N-Q=O LUMOPr-N-Q=O

Figure 3. Schematic representations of HOMO and LUMO molecular orbitals of studied molecules of Pr-N-Q=S and Pr-N-Q=O calculated in solvent phase (water) at the B3LYP/6-31G(d,p) level.

According to the frontier molecular orbital theory (FMO) of chemical reactivity, transition of electron is due to interaction between the HOMO and the LUMO of the reacting species [65]. The energy of the highest occupied molecular orbital (E_{HOMO}) measures the predisposition towards the donation of electron by a molecule. Consequently, higher values of E_{HOMO} designate better propensity towards the donation of electron, increasing the adsorption of the inhibitor on mild steel and then better inhibition efficiency. E_{LUMO} specifies the capacity of the molecule to receive electrons. The binding aptitude of the inhibitor to the metal surface growths with increasing of the HOMO and decreasing of the LUMO energy values.The quantum chemical descriptors are frequently associated with the electron donating ability of the molecule. We have calculated and gathered in Table 4, the quantum chemical parameters most relevant to the potential action as corrosion inhibitors such as E_{HOMO} (highest occupied molecular orbital energy), E_{LUMO} (lowest unoccupied molecular orbital energy), energy gap (ΔE), dipole moment (μ), electron affinity (AE), ionization potential (IP), absolute electronegativity (χ), global hardness (η), softness (S), fraction of electrons transferred (ΔN), electrophilicity index (ω) and back-donation ($\Delta E_{back\text{-}donation}$) for the molecules Pr-N-Q=S and Pr-N-Q=O in solvent phase (water) with the DFT at the B3LYP/6-31G(d,p) level.

Table 4. Quantum chemical parameters for the molecules Pr-N-Q=S and Pr-N-Q=O obtained in solvent phase (water) with the DFT at the B3LYP/6-31G(d, p) level.

Quantum Chemical Parameters	Pr-N-Q=S	Pr-N-Q=O
E_{LUMO} (eV)	-2.4322	-1.8849
E_{HOMO} (eV)	-6.0856	-6.2842
ΔE (eV)	3.6534	4.3993
IP (eV)	6.0856	6.2842
EA (eV)	2.4322	1.8849
χ (eV)	4.2589	4.0846
η (eV)	1.8267	2.1996
μ (debye)	6.5708	4.0635
ω (eV)	11.8179	3.7534
S $(eV)^{-1}$	0.5474	0.4546
ΔN	0.7503	0.6627
$\Delta E_{back\text{-}donation}$ $(eV)^{-1}$	-0.4567	-0.5499
Total energy (a.u)	-970.9512	-647.9962

When we compare the two compounds Pr-N-Q=S and Pr-N-Q=O, the calculations show that the compound Pr-N-Q=S has the highest HOMO level at −6.0856 eV and the lowest LUMO level at −2.4322 eV. Thus the values of E_{HOMO} and E_{LUMO} are in conformity with the trend of inhibition efficiency (Pr-N-Q=S is the best inhibitor among the two quinoxaline derivatives). Thus, the highest inhibition efficiency of Pr-N-Q=S is due to the increasing energy of the HOMO and the decreasing energy of the LUMO. This is in good agreement with the experimental observations suggesting that the inhibitor Pr-N-Q=S has the highest inhibition efficiency.

Energy band Gap (ΔE_{gap}) is an essential parameter which provides a measure for the stability of the inhibitor molecule towards the adsorption on metallic surface (physisorption& chemisorption). In this work, Pr-N-Q=S showed good inhibitory effect against the corrosion of iron in hydrochloric acid solution and is considered to be the most effective. The results obtained in Table 4 demonstrate that the compound Pr-N-Q=S has the lowest ΔE_{gap} (3.6534 eV); this means that the molecule could have better performance as corrosion inhibitor. This is in good agreement with the experimental observations. In fact, as ΔE_{gap} decreases, the reactivity of the molecule increases leading to increase the inhibition efficiency of the molecule.

Ionization energy (IE) is an important descriptor of the chemical reactivity of atoms and molecules. High ionization energy designates high stability and chemical inertness and small ionization energy specifies high

reactivity of the atoms and molecules [66]. The low ionization energy (IE = 6.0856 eV) of Pr-N-Q=S indicates the high inhibition efficiency. This is in good agreement with the experimental observations.

The absolute electronegativity (χ) is the chemical property that describes the ability of a molecule to attract electrons towards itself in a covalent bond. According to Sanderson's electronegativity equalization principle [67], the molecule Pr-N-Q=S with a high electronegativity quickly reaches equalization and hence low reactivity is expected which in turn indicates low inhibition efficiency. The Table 4 shows that the highest electronegativity is encountered for Pr-N-Q=S. Hence an increase in the difference of electronegativity between the metal and inhibitor is observed at the largest extent for Pr-N-Q=S. This is in good agreement with the experimental results.

Absolute hardness (η) and Softness (σ) are essential properties to measure the molecular stability and reactivity. It is apparent that the chemical hardness fundamentally indicates the resistance towards the deformation or polarization of the electron cloud of the atoms, ions or molecules under small perturbation of chemical reaction. A hard molecule has a great energy gap and a soft molecule has a small energy gap [68]. In our present study Pr-N-Q=S with low hardness value 1.8267 eV compared with other compound have a low energy gap. Normally, the inhibitor with the least value of global hardness (hence the highest value of global softness) is expected to have the highest inhibition efficiency [69]. For the simplest transfer of electron, adsorption could occur at the part of the molecule where softness (σ), which is a local property, has a highest value [68]. Pr-N-Q=S with the softness value of 0.5474 eV has the highest inhibition efficiency. This is in good agreement with the experimental observations.

Dipole moment, μ(Debye), is another important electronic parameter that results from non-uniform distribution of charges on the various atoms in the molecule [70]. The high value of μ (Debye) probably increases the adsorption between the chemical compound and the metal surface [71]. The energy of the deformability increases with the increase in μ, making the molecule easier to adsorb at the iron (Fe) surface. The volume of the inhibitor molecule Pr-N-Q=S also increases with the increase of μ. This increases the contact area between the molecule and the surface of iron and increases the corrosion inhibition ability of the inhibitor. In our study, among the two quinoxaline derivatives, the dipole moment for Pr-N-Q=S is the highest (6.5708 Debye). Thus, there is a direct relationship between the inhibition efficiency and the dipole moment.

When considering the global electrophilicity index (ω) which is the measure of the electrophilic tendency of a molecule, we find that the inhibitor Pr-N-Q=S with high electrophilicity index value (11.8179 eV) than the other compounds, has the highest inhibition efficiency. This result is in good agreement with the experiment.

The calculated values of the Number of electrons transferred (ΔN) show that the inhibition efficiency resulting from electron donation agrees with Lukovit's study [72]. If $\Delta N < 3.6$, the inhibition efficiency increases by increasing electron- donating ability of these inhibitors to donate electrons to the metal surface. The results indicate that ΔN values correlates strongly with experimental inhibition efficiencies. Thus, the highest fraction of electrons transferred (0.7503) is associated with the best inhibitor Pr-N-Q=S. This is in good agreement with the experimental observations.

The calculated values of $\Delta E_{back\text{-}donation}$ for the inhibitors under study as listed in Table 4 reveal that the highest value of $\Delta E_{back\text{-}donation}$ is encountered for Pr-N-Q=S, which indicates that back-donation is favored for the Pr-N-Q=S molecule which is the best inhibitor. This is in good agreement with the experimental results.

Total energy calculated by quantum chemical methods is also a beneficial parameter. The total energy of a system is composed of the internal, potential, and kinetic energy. Hohenberg and Kohn proved that the total energy of a system including that of the many body effects of electrons in the presence of static external potential is a unique functional of the charge density [73]. The minimum value of the total energy functional is the ground state energy of the system. The electronic charge density, which yields this minimum, is then the exact single particle ground state energy. In our study the total energy of the best inhibitor Pr-N-Q=S is equal to -970.9512 eV; this value is the lowest for the two molecules under study. This is in good agreement with the experimental findings.

In this work, Mulliken population analysis is carried out to determine the electron rich groups/atoms for the molecules under study and is therefore used to evaluate the adsorption centres of inhibitors since this method has been generally reported and it is commonly used for the calculation of the charge distribution over the entire

skeleton of the molecule [74]. There is a general unanimity by many authors that the more negatively charged heteroatom is, the more is its ability to absorb on the metal surface through a donor-acceptor type reaction [75]. Variation in the inhibition efficiency of the two inhibitors under study depends on the presence of electronegative Sulphur, Oxygen and Nitrogen atoms in their molecular structure. The site of ionic reactivity could be estimated from the net charges on a molecule. Table 5 representing the effective atomic charges from Mulliken populations of Pr-N-Q=S and Pr-N-Q=O inhibitors in aqueous solution, shows that Sulphur, Oxygen and Nitrogen atoms and some carbon atoms carry more negative charges, while the remaining carbon atoms carry more positive charges. This means that the atoms carrying negative charges are the negative charge centres, which can offer electrons to the Fe atoms to form coordinate bond, and the atoms carrying positive charges are the positive charge centres, which can accept electrons from orbital of Fe atoms to form feedback bond.

The calculated Mulliken charges at the B3LYP/6-31G(d, p) level for the molecules Pr-N-Q=S and Pr-N-Q=O are in good agreement with the delocalization of charges, leading to an excess of negative charges on the Sulphur, Oxygen and Nitrogen atoms. We emphasize also that the highest negative charges were found for the heteroatoms while the highest positive charges were found for some Carbon atoms. These findings are attributed to the electronegativity of Sulphur, Oxygen and Nitrogen atoms. Besides, some Carbon atoms bear significant negative charges. This delocalization character of electrons yields to quinoxaline stable planar structures. Thus, the optimized structure is in accordance with the fact that excellent corrosion inhibitors cannot only offer electrons to unoccupied orbital of the metal, but also accept free electrons from the metal. Therefore, it can be inferred that quinoxaline ring, the oxo group or thioxo group are the possible active adsorption sites. We emphasize that the charge gradient is maximum, in Pr-N-Q=S, for the Sulphur atom with the Carbon atom in the thioxo group (-0.3344 for S25 and 0.1447 for C11). Conversely, weak charge gradients are encountered for Pr-N-Q=O (-0.5648 for O14 and 0.5931 for C11). These findings corroborates the experimental results, where among the two quinoxaline derivatives under study, Pr-N-Q=S is the best inhibitor.

Table 5. Calculated Mulliken atomic charges for heavy atoms of Pr-N-Q=S and Pr-N-Q=O in solvent phase using DFT at the B3LYP/6-31G (d.p) basis set.

Pr-N-Q=S		**Pr-N-Q=O**	
C1	-0.0961	**C1**	-0.1029
C2	-0.1059	**C2**	-0.1128
C3	0.2358	**C3**	0.2199
C4	0.3563	**C4**	0.3586
C5	-0.1145	**C5**	-0.1263
C6	-0.1035	**C6**	-0.1056
C11	0.1447	**C11**	0.5931
C12	0.2726	**C12**	0.2391
N13	-0.5088	**N13**	-0.5777
C14	-0.2252	**O14**	-0.5648
C17	-0.3615	**C15**	-0.2120
N21	-0.5250	**C18**	-0.3619
C22	0.2990	**N22**	-0.5372
C23	-0.4084	**C23**	0.2842
S25	-0.3344	**C24**	-0.4182

From the theoretical calculations carried on the inhibitors molecular systems in solvent phase (water) with the DFT at B3LYP/6-31G(d,p) level, high correlation coefficients of the inhibition efficiencies with electronic properties was obtained. Therefore, theoretical calculations on these molecules could be a good approach for the study of their potential inhibition capability of metal corrosion in hydrochloric acid.

3.2. Monte Carlo simulations

In the current study, the MC simulation was performed to study the behavior of the system (single inhibitor molecule / iron surface) in water as solvent. The single molecules of (Pr-N-Q=O and Pr-N-Q=S) on Fe (111) surface configuration are sampled from a canonical ensemble. The total energy, Van der Waals energy, average total energy, electrostatic energy and intermolecular energy for the systems under study; Fe (111) / (Pr-N-Q=O and Pr-N-Q=S)in water as solvent are calculated by optimizing the whole system and given in Figure 4.The most stable low energy adsorption configurations of the inhibitors (Pr-N-Q=O and Pr-N-Q=S) adsorbed onto the iron (111) surface in water solvent molecules (30 H_2O) using Monte Carlo simulations are depicted in Figure 5. Side and top views of stable adsorption configurations for the inhibitors under study on Fe(111) / 30 H_2O system using Monte Carlo simulations are given in Figure 5.

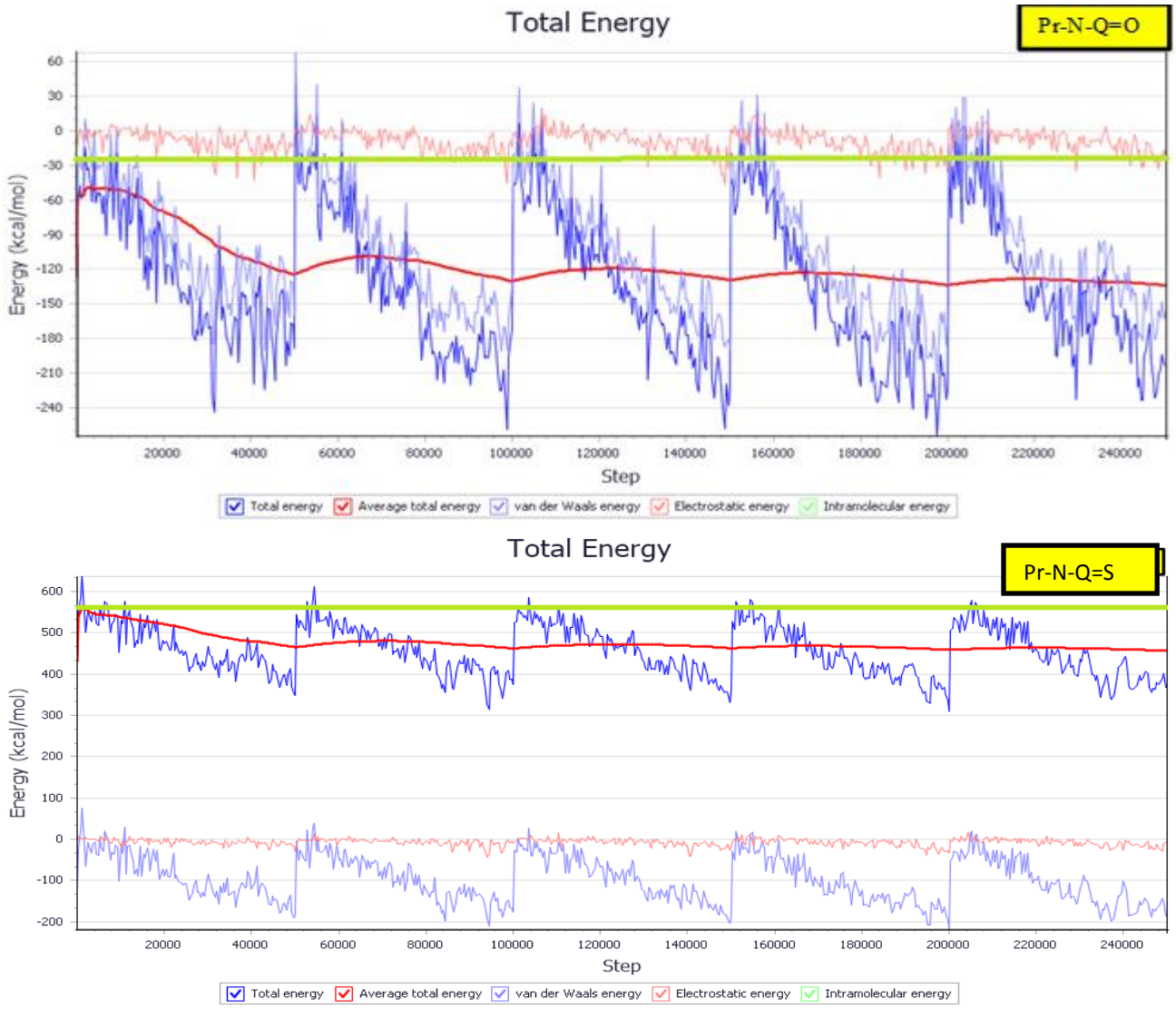

Figure 4. Total energy distribution for Fe (111) / (Pr-N-Q=O and Pr-N-Q=S) / 30 H_2O complexes during energy optimization process.

From Figure 5 we show that the adsorption centers of all inhibitors on the iron (111) surface in water solvent molecules are the π-electrons of quinoxaline ring, nitrogen (-N=), oxygen (-O-) and sulfur (-S-) heteroatoms. For the Pr-N-Q=O and Pr-N-Q=S inhibitor molecules, the calculated dihedral angles around the quinoxaline ring are close to 0° or 180°, indicating planarity of the quinoxaline ring. Thus, thePr-N-Q=O and Pr-N-Q=S inhibitor molecules adsorbed nearly plane on the iron (111) surface in water solvent molecules to maximize surface coverage and contact (Figure 5), ensuring a strong interaction between adsorbate and substrate. This finding is in good agreement with our experimental results.

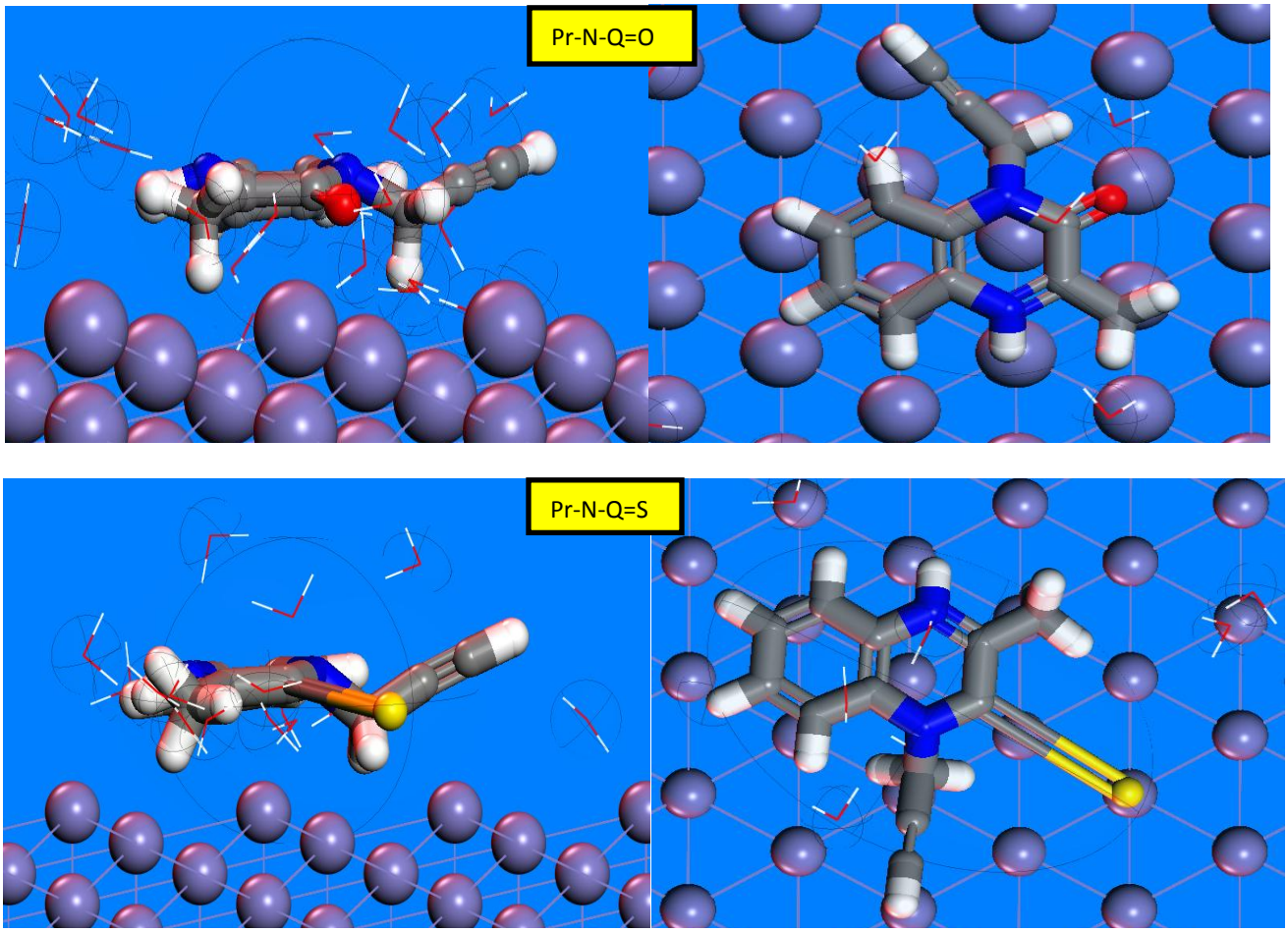

Figure 5. Side and top views of stable adsorption configurations for Fe (111) / (Pr-N-Q=O and Pr-N-Q=S)/ 30 H_2O complexes obtained using the Monte Carlo simulations.

The values for the outputs and descriptors calculated by the Monte Carlo simulations for Fe (111) / (Pr-N-Q=S and Pr-N-Q=O)/ 30 H_2O systems are listed in Table 6. The parameters presented in Table 6 include total energy (E_{Total}), in Kcal/mol, of the substrate–adsorbate configuration. The total energy is defined as the sum of the energies of the adsorbate components. The total energy of the inhibitors on iron surface in the presence of water follows the trend: Pr-N-Q=S <Pr-N-Q=O. Hence, the inhibitor Pr-N-Q=S is the most stable among the two inhibitors.

The adsorption energy(E_{Ads}), in Kcal/mol, reports energy released (or required) when the relaxed adsorbate components (Pr-N-Q=O and Pr-N-Q=S) are adsorbed onto the substrate (Fe (111) surface). It is commonly recognized that the main mechanism of corrosion inhibitor interaction with steel is by adsorption. Therefore, the adsorption energy may help us to rank inhibitor molecules [76-77]. From Table 6, it is quite clear that the adsorption energies values are negative, which denote that the adsorption could occur spontaneously [78].

Table 6. Outputs and descriptors for the lowest adsorption configurations for Fe (111) / (Pr-N-Q=O and Pr-N-Q=S) / 30 H_2O systems calculated by Monte Carlo simulation. (All values are given in Kcal/mol).

Inhibitors	E_{Total}	E_{Ads}	R.A.E	D_{Energy}	dE_{ads}/dN_i Inhs	dE_{ads}/dN_i Water
Pr-N-Q=O	-428.85	-417.31	-418.05	0.74	-117.06	-5.71
Pr-N-Q=S	-478.56	-1039.06	-432.39	-606.67	-719.05	-5. 94

The adsorption energy of the Pr-N-Q=S inhibitor (-1039.06 Kcal/mol) is the highest negative value among the inhibitors under study, which means that adsorption of Pr-N-Q=S molecule on iron (111) surface in water solvent molecules is stronger than Pr-N-Q=O. This is due to the presence of electron donating group (-C≡CH) attached to quinoxaline ring on the structure, which serves as additional active centres and also to the existence of thioxo group on the quinoxaline ring, which gives the possibility of dπ-dπ bond formation resulting from overlap of 3d electrons from Fe atom and the 3d vacant orbital of sulphur atom [62-64].The adsorption energies of the inhibitors on iron surface in the presence of water decreased in the order: Pr-N-Q=S >Pr-N-Q=O. This ordering shows that the system with the most stable and stronger adsorption is Fe (111) / Pr-N-Q=S. Hence, Pr-N-Q=S is the best corrosion inhibitor among the two inhibitors under study. Besides, the high negative value for the adsorption energy of the Pr-N-Q=S inhibitor is in good agreement with the experimental results showing that the adsorption mechanism of the inhibitor Pr-N-Q=S on mild steel surface in 1 M HCl solution as typical of chemisorption [79]. In fact, a high negative adsorption energy will designates the system with the most stable and stronger adsorption [80-81]. Moreover, the chemisorption is favoured by the Pr-N-Q=S planarity demonstrated by our Monte Carlo simulations. Conversely, the low negative value for the adsorption energy of the other inhibitor Pr-N-Q=O is also in good agreement with the experiment where we have demonstrated that the adsorption mechanism, of this inhibitor, on mild steel surface in 1 M HCl solution involves physisorption [61, 82]. Therefore our Monte Carlo results are in good agreement with the experiment where the inhibition efficiency (IE) for inhibitor Pr-N-Q=S is the highest. The observed trend experimentally (Pr-N-Q=S >Pr-N-Q=O) is consistent with our Monte Carlo results.

In this work, the substrate energy is taken as zero. The adsorption energy is defined as the sum of the rigid adsorption energy (R.A.E) and the deformation energy for the adsorbate components. The rigid adsorption energy reports the energy, in Kcal/mol, released (or required) when the unrelaxed molecules, (Pr-N-Q=S and Pr-N-Q=O) before the geometry optimization step are adsorbed on the iron (111) surface in presence of 30 molecules of water. The deformation energy (D_{Energy}) reports the energy, in Kcal/mol, released when the adsorbed component molecule (Pr-N-Q=S and Pr-N-Q=O) is relaxed on the iron surface. Table 6 shows also (dE_{ads}/dN_i), which reports the energy, in Kcal/mol, of Fe–components configurations (Pr-N-Q=S and Pr-N-Q=O) where one of the inhibitor molecules has been removed.

Conclusions

Our previous experimental results for two quinoxaline derivatives were supported, in the present work, with that obtained by means of the first principles theoretical calculations using the computational methodologies of quantum chemistry. The inhibitor efficiencies of these compounds seem to be determined by the conjugation of electronic factors and molecular geometry. The analysis of the HOMO, LUMO, and partial atomic charges suggests the centres that would be preferred for nucleophilic or electrophilic attack. The DFT calculations correlate strongly with experimental results and indicate that PR-N-Q=S had a stronger interaction with the steel than the other quinoxaline derivatives thanks to the existence of thioxo group on the quinoxaline ring, which gives the possibility of dπ-dπ bond formation resulting from overlap of 3d electrons from Fe atom and the 3d vacant orbital of sulphur atom. Through DFT quantum-chemical calculations a correlation between, parameters associated to the electronic structure of two quinoxaline derivatives and their potential to inhibit the corrosion process, could be established. The calculated molecular parameters in the neutral form of the inhibitors calculated with the DFT at the B3LYP/6-31G(d,p) level show excellent correlation with inhibition efficiency of the

inhibitors studied, confirming the reliability of the method employed. We have demonstrated using Monte Carlo simulations that the order of adsorption of the inhibitors under study on iron surface agrees with the experimental trend (Pr-N-Q=S and Pr-N-Q=O). The inhibitor Pr-N-Q=S has the strongest interaction with the steel surface than the other inhibitor, which corroborate very well with our experimental results. We emphasize, on the one hand, that the adsorption mechanism of the Pr-N-Q=S on mild steel surface is typical of chemisorption which agrees with our experimental finding and on the other hand, that the adsorption mechanism of the Pr-N-Q=O on mild steel surface are typical of physisorption which approves our experimental results.

Acknowledgments-Y.K. appreciates the Laboratory for Chemistry of Novel Materials,University of Mons, Belgium, for the access to the computational facility.

References

1. Ahmad N., MacDiarmid A. G., *Synthetic Metals.* 78 (1996) 103-110.
2. Belghiti ME., Tighadouini S., Karzazi Y., Dafali A., Hammouti B., Radi S., Solmaz R., *J. Mater. Environ. Sci.*, 7 (1) (2016) 337-346.
3. BelghitiM.E., Karzazi Y., Tighadouini S., Dafali A., Jama C., Warad I., Hammouti B., Radi S., *J. Mater. Environ. Sci.*, 7 (3) 956-967, 2016.
4. Mercer A.D., Corrosion Inhibition: Principles and Practice, Oxford, UK, Butterworths Heinemann (1994).
5. Umoren S.A., Li Y., Wang F.H., *Corros. Sci.*, 52 (2010) 1777-1786.
6. Speight J. G., Chapter 6, Corrosion Monitoring and Control Oil and Gas Corrosion Prevention, (2014) 109-149.
7. Sastri VS., Corrosion Inhibitors: Other Important Applications Reference Module in Materials Science and Materials Engineering, from Shreir's Corrosion, 4 (2010) 2990-3000.
8. McIntyre PJ., Mercer AD., Corrosion Testing and Determination of Corrosion Rates, Reference Module in Materials Science and Materials Engineering, from Shreir's Corrosion, 2 (2010) 1443-1526.
9. Kertit S., Hammouti B., *Appl. Surf. Sci.* 93 (1) (1996) 59-66.
10. Zhang S., Tao Z., Liao S., Wu F., *Corros. Sci.*, 52 (2010) 3126-3132.
11. Anusuya N., Sounthari P., Saranya J., Parameswari K., Chitra S., *J. Mater. Environ. Sci.*, 6 (6) (2015) 1606-1623.
12. Khadraoui A., Khelifa A., Boutoumi H., Karzazi Y., Hammouti B., Al-Deyab S.S., *Chemical Engineering Communications*, 203 (2) (2016) 270-277,
13. Zarrouk A., Zarrok H., Ramli Y., Bouachrine M., Hammouti B., Sahibed-dine A., Bentiss F., *Journal of MolecularLiquids*, 222 (2016) 239-252.
14. Jafari H., mohsenifar F., Sayin K., *J. Taiwan Inst. Chem. Eng.*, 64 (2016) 314-324.
15. Anejjar A., Salghi R., Jodeh S., Karzazi Y., Warad I., Dassanayake R., Hamed O., Zarouk A., Hammouti B., *Magh. J. Pure and Appl. Science.*, 1 (1) (2015) 25-42.
16. Bousskri A., Anejjar A., Messali M., Salghi R., Benali O., Karzazi Y., Jodeh S., Zougagh M., Ebenso E.E., Hammouti B., *Journal of Molecular Liquids.*, 211 (2015) 1000-1008,.
17. Lagrenee M., Mernari B., Chaibi N., Traisnel M., Vezin H and Bentiss F., *Corros. Sci.*, 43 (2001) 951.
18. Chetouani A. &Hammouti B., Molecular modelling Quantum Chemical Studies and Corrosion Inhibitors - Synthesis and Use of New Heterocyclic and polymers for the Protection of Steel in Acid Medium, ISBN: 978-3-659-39805-6, Lambert Academic Publishing., (2013) 1-167.
19. Aouniti A., Khaled K.F., Hammouti B., *Int. J. Electrochem. Sci.*, 8 (2013) 5925-5943.
20. Krim O., Elidrissi A., Hammouti B., Ouslim A., Benkaddour M., *Chem. Eng. Comm.*, 196 (12) (2009) 1536-1546.
21. Sulaiman KO., A. T. Onawole *Computational and Theoretical Chemistry*, 1093 (2016) 73-80.
22. Zarrouk A., El Ouali I., Bouachrine M., Hammouti B., Ramli Y., EssassiEM., Warad I., Aouniti A., Salghi R., *Res. Chem. Intermed.*, 38 (2013) 1125-1133.
23. Zarrok H., Zarrouk A., Salghi R., Elmahi B., Hammouti B., Al-Deyab S.S., EbnTouhami M., Bouachrine M., Oudda H., Boukhris S., *Int. J. Electrochem. Sci.*, 8 (2013) 11474-11491.

24. Zarrouk A., Bouachrine M., Hammouti B., Dafali A., Zarrok H., *J. SaudiChem. Soc.* 18 (5) (2014) 550-555.
25. Zarrouk A., Zarrok H., Ramli Y., Bouachrine M., Hammouti B., Sahibed-dine A., Bentiss F., *Journal of Molecular Liquids*, 222 (2016) 239-252.
26. Loriga M., Piras S., Sanna P., G. Paglietti, *Farmaco.*, 52 (1997) 157.
27. Seitz L.E., SulingW.J., Reynolds R.C., *J. Med. Chem.*, 45 (2002) 5604.
28. Yb K., Yh K., Jy P., SK K., *Bioorg. Med. Chem. Lett.*, 14 (2004) 541.
29. Hui X., Desrivot J., Bories C., Loiseau P.M., Franck X., Hocquemiller R., Figadere B., *Bioorg. Med. Chem. Lett.*, 16 (2006) 815.
30. Lindsley C.W., Zhao Z., Leister W.H., Robinson R.G., Barnett S.F., Defeo-Jones D., Jones R.E., Hartman G.D., Huff J.R., Huber H.E., Duggan M.E., *Bioorg. Med. Chem. Lett.*, 15 (2005) 761.
31. Labarbera D. V., SkiboE.B., *Bioorg. Med. Chem.*, 13 (2005) 387.
32. Sarges R., Howard HR., Browne R.G., Lebel LA., Seymour PA., Koe BK., *J. Med. Chem.*, 33 (1990) 2240.
33. Srinivas C., Kumar CNSSP., Rao VJ., Palaniappan S., *Journal of Molecular Catalysis A: Chemical* 265 (1) (2007) 227-230.
34. Ghomsi NT., AhabchaneNEH., Es-Safi NE., Garrigues B., Essassi El M., *SpectroscopyLett.*, 40 (2007) 741.
35. Sakata G., Makino K., Karasawa Y., *Heterocycles* 27 (1988) 2481.
36. Karzazi Y., Belghiti M.E., Dafali A., Hammouti B., J. Chem. Pharm. Res. 6 (2014) 689-696.
37. Khadraoui A., Khelifa A., Boutoumi H., Mettai B., Karzazi Y., Hammouti B., *Portugaliae Electrochim. Acta* 32 (4) (2014) 271-280.
38. Belghiti M.E., Dahmani M., Messali M., Karzazi Y., Et-Touhami A., Yahyi A., Dafali A., Hammouti B., *Der Pharma Chemica*, 7 (5) (2015) 106-115.
39. Becke A.D., *J. Chem. Phys.* 96 (1992) 9489-9497.
40. Becke A.D., *J. Chem. Phys.* 98 (1993) 1372-1377.
41. Lee C., Yang W., Parr R.G., Phys. Rev. B 37 (1988) 785-789.
42. Frisch MJ., Trucks GW., Schlegel HB., Scuseria GE., Robb MA., Cheeseman JR., Scalmani G., Barone V., Mennucci B., Petersson GA., Nakatsuji H., Caricato M., Li X., Hratchian H. P., Izmaylov, J. Bloino AF., Zheng G., Sonnenberg JL., Hada M., Ehara M., Toyota K., Fukuda R., Hasegawa J., Ishida M., Nakajima T., Honda Y., Kitao O., Nakai H., Vreven T., Montgomery J. A., Jr., Peralta J. E., Ogliaro F., Bearpark M., HeydJJ., Brothers E., Kudin KN., Staroverov VN., Kobayashi R., Normand J., Raghavachari K., Rendell A., Burant JC., Iyengar SS., Tomasi J., Cossi M., Rega N., Millam JM., Klene M., Knox JE., Cross JB., Bakken V., Adamo C., Jaramillo J., Gomperts R., Stratmann RE., Yazyev O., Austin AJ., Cammi R., Pomelli C., OchterskiJW., Martin RL., Morokuma K., Zakrzewski VG., Voth GA., Salvador P., Dannenberg JJ., Dapprich S., Daniels AD., Farkas Ö., Foresman JB., Ortiz JV., Cioslowski J., Fox DJ., Gaussian, Inc. Wallingford CT, (2009).
43. Tomasi J., Mennucci B., Cammi R., *Chem. Rev.*, 105 (2005) 2999-3093.
44. Domenicano A., Hargittai I., Accurate Molecular Structures, Their Determination and Importance, Oxford University Press., New York, 1992.
45. Li W., Zhao X., Liu F., Deng J., Hou B., *Mater. Corros.*, 60 (2009) 287-293.
46. Saha SKr., Ghosh P., Chowdhury AR., Samanta P., Murmu NC., Lohar AKr., Banerjee P., *Can. Chem. Trans.*, 2 (2014) 381-402.
47. Wang H., Wang X., Wang H., Wang L., Liu A., *J. Mol. Model.*, 13 (2007) 147-153.
48. Fleming I., Frontier Orbitals and Organic Chemical Reactions, John Wiley and Sons, New York, 1976.
49. Parr RG., Szentpaly L., Liu S., *J. Am. Chem. Soc.* 121 (1999) 1922-1924.
50. Sastri VS., Perumareddi JR., *Corros. Sci.* 53 (1997) 617-622.
51. Morad MS., *Corros. Sci.* 50 (2008) 436–448.
52. DewardMJS., Thiel W., *J. Am. Chem. Soc.* 99 (1977) 4899-4907.
53. Gomez B., LikhanovaNV., Dominguez-Aguilar MA., Vela R., Martinez-Palou A., Gasquez J., *J. Phys. Chem.* B 110 (2006) 8928-8934.
54. Metropolis N., Rosenbluth AW., Rosenbluth MN., Teller AH., Teller E., *J. Chem. Phys.* 21 (1953) 1087.
55. Delley B., *J. Chem. Phys.* 92 (1990) 508.

56. Delley B., *J. Chem. Phys.* 113 (2000) 7756.
57. Frenkel D., Smit B., Understanding Molecular Simulation: From Algorithms to Applications, 2nd Edition, Academic Press, San Diego (2002).
58. Kirkpatrick S., Gelatt CD., Vecchi MP., *Science*, 220 (4598) (1983) 671-680.
59. BIOVIA Materials Studio version 8.0, Accelrys Inc. USA., 2014.
60. Sun H., *J. Phys. Chem.*, B102 (1998) 7338-7364.
61. El-Hajjaji F., Zerga B., Sfaira M., Taleb M., EbnTouhami M., Hammouti B., Al-Deyab S.S., H. Benzeid, Essassi El M., *J. Mater. Environ. Sci.* 5 (1) (2014) 255-262.
62. El Adnani Z., Mcharfi M., Sfaira M., Benjelloun A.T., Benzakour M., EbnTouhami M., Hammouti B., Taleb M., *Int. J. Electrochem. Sci.*, 7 (2012) 3982.
63. El Adnani Z., Mcharfi M., Sfaira M., Benzakour M., Benjelloun A.T., EbnTouhami M., Hammouti B., Taleb M., *Int. J. Electrochem. Sci.*, 7 (2012) 6738.
64. El Adnani Z., Mcharfi M., Sfaira M., Benzakour M., Benjelloun A.T., EbnTouhami M., *Corros. Sci.*, 68 (2013) 223.
65. Musa A.Y., Kadhum A.H., Mohamad A.B., Rohoma A.B., Mesmari H., *J. Mol. Struct.* 969 (2010) 233-237.
66. SandipK.R., Nazmul I., DulalC.G., *J. Quant. Infor. Sci.* 1 (2011) 87-95.
67. Geerlings P., De Proft F., *Int. J. Mol. Sci.* 3 (2002) 276-309.
68. Hasanov R., Sadikglu M., Bilgic S., *Appl. Surf. Sci.*, 253 (2007) 3913.
69. Ebenso E.E., Isabirye D.A., Eddy N.O., *Int. J. Mol. Sci.*, 11 (2010) 2473-2498.
70. Kikuchi O., *Quant. Struct. Act. Relat.*, 6 (1987) 179-184.
71. Li X., Deng S., Fu H., Li T., *Electrochim. Acta* 54 (2009) 4089-4098.
72. Lukovits I., Kalman E., Zucchi F., *Corrosion* 57 (2001) 3-8.
73. Ju H., Kai Z.P., Li Y., *Corros. Sci.*, 50 (2008) 865-871.
74. Saha SKr., Ghosh P., Hens A., Murmu NC., Banerjee P., *Phys. E.* 66 (2015) 332–341.
75. Saha SKr., Dutta A., Ghosh P., Sukul D., Banerjee P., *Phys. Chem. Chem. Phys.* 17 (2015) 5679–5790
76. Belghiti ME., Karzazi Y., Dafali A., Hammouti B., Bentiss F., ObotIB., Bahadur I., Ebenso EE., *J. Mol. Liq.*, 218 (2016) 281-293.
77. Belghiti ME., Karzazi Y., Dafali A., Obot I.B., Ebenso EE., Emrane KM., Bahadur I., Hammouti B., Bentiss F., *J. Mol. Liq.*, 216 (2016) 874-886.
78. EbensoEE., Kabanda MM., Arslan T., Saracoglu M., Kandemirli F., UrulanaLC., Singh AK., Shukla SK., Hammouti B., Khaled KF., Quraishi MA., Obot IB., Eddy NO., *Int. J. Electrochem. Sci.*, 7 (2012) 5643-5676.
79. El-Hajjaji F., Belkhmima R.A., Zerga B., Sfaira M., Taleb M., Ebn Touhami M., Hammouti B., Al-Deyab S.S., Ebenso EE., *Int. J. Electrochem. Sci.*, 9 (2014) 4721-4731.
80. Obot I. B., Umoren S.A., Gasem Z.M., Suleiman R., El Ali B., *J. Ind. Eng. Chem.*, 21 (2015) 1328-1339.
81. Kumar A. M., Babu R. S., Obot I. B., Gasem Z.M., *RSC Adv.*, 5 (2015) 19264-19272.
82. El-Hajjaji F., Belkhmima R.A., Zerga B., Sfaira M., Taleb M., Ebn Touhami M., Hammouti B., *J. Mater. Environ. Sci.*, 5 (1) (2014) 263-270.